Variations of Total Hemoglobin Concentration in Forearm Muscles Caused by Vascular Occlusions and Monitored by Near-Infrared Spectroscopy: A Novel Electrical Model

Vo Van Toi, Matthew Hoimes, Shalini Nadgir, and Sergio Fantini
Tufts University, Department of Biomedical Engineering, Medford, MA 02155

Abstract

We propose an electrical model to describe the hemodynamic changes induced by a venous occlusion in a human limb. To test the model, we have performed NIRS measurements on the human forearm, specifically on the brachioradialis muscle, during venous occlusion induced by a pneumatic cuff inflated around the upper arm to pressures within the range 5-60 mmHg. We have found a good qualitative agreement between parameters measured by NIRS (total hemoglobin concentration and hemoglobin saturation) and the corresponding model parameters (capacitor voltage and venous-branch current). These results indicate that this electrical model can be a valuable analytical tool to characterize, optimize, and further develop diagnostic measurement schemes that use venous occlusion approaches.

Introduction

Electrical models have been commonly used to study and describe the vascular system using resistors to represent vascular resistance, capacitors for compliance, and inductors for inertance [Westerhof et al. 1971; Stergiopulos et al. 1999; Olufsen et al. 2002, Voytik et al. 1990; Babbs et al. 1984; Olmi et al. 1998, Sainz et al 1995].

Near-infrared spectroscopy (NIRS) is a non-invasive technique for the functional and metabolic study of tissue. The absorption of near-infrared light in tissue is mainly due to hemoglobin in its oxygenated (HbO_2) and deoxygenated (Hb) forms. Spectral measurements allow for the separate determination of the concentrations of these two species ($[HbO_2]$ and [Hb]) in tissue, which lead to the total hemoglobin concentration (THC = $[HbO_2]$ + [Hb]) and hemoglobin saturation (StO_2 = $[HbO_2]$/THC). THC and StO_2 are indicative of the balance between the local blood flow, blood volume, and oxygen utilization rate, which are relevant physiological and metabolic parameters.

Reported investigations of the hemodynamics of the forearm and calf muscles using NIRS indicated that when the pressure reached a threshold value (about 30mmHg) the venous outflow was hindered and when it reached a critical value (between 30 and 45 mmHg) the complete occlusion occurred. Further, if the pressure increased from 30 mmHg to 45 mmHg in less than 6 seconds the blood flow and oxygen consumption were independent of the total inflation time and final cuff pressure (Casavola et al.). It was also reported that the venous occlusion happened in an on-off manner i.e., the blood flow is abruptly interrupted when the externally applied pressure reaches a certain critical value (de Blasi et al.). In this study, we have experimentally investigated the dependence of the THC measured in the forearm in response to a vascular occlusion in the upper arm, and we propose an electrical model to describe the hemodynamic response to occlusion.

Materials and methods

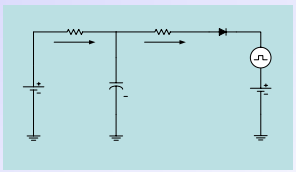

Fig. 1: Electrical model
The proposed electrical model for the hemodynamic changes induced by venous occlusion. The voltage sources V_{art}, V_v, and v_{ext} model the arterial, venous, and cuff pressures, respectively, whereas i_a and i_v represent the arterial and venous blood flow, respectively. The vascular resistance is modeled by resistors R_a and R_v, while the effects of vascular compliance and capillary recruitment are modeled by capacitor C. The ideal diode D imposes that i_a and i_v never flow in the direction opposite to that indicated by the arrows.

Table 1: *Analytical expressions for the circuit model for "small" rectangular wave V_{ext}. ($V_{ext} < V_{crit}$)*

	$t<t_1$	$t_1 \le t < t_2$	$t \ge t_2$
$i_a(t)$	$I_a^{(rest)}$	$\left[I_a^{(rest)} - I_a^{(occl)}\right]e^{-(t-t_1)/\tau_1} + I_a^{(occl)}$	$\left[i_a(t_2^-) - I_a^{(rest)}\right]e^{-(t-t_2)/\tau_1} + I_a^{(rest)}$
$i_v(t)$	$I_v^{(rest)}$	$\left[I_v^{(rest)} - \frac{V_{ext}}{R_v} - I_v^{(occl)}\right]e^{-(t-t_1)/\tau_1} + I_v^{(occl)}$	$\left[i_v(t_2^-) - I_v^{(rest)}\right]e^{-(t-t_2)/\tau_1} + I_v^{(rest)}$
$v_C(t)$	$V_a - R_a I_a^{(rest)}$	$R_a\left[I_a^{(occl)} - I_a^{(rest)}\right]e^{-(t-t_1)/\tau_1} + V_a - R_a I_a^{(occl)}$	$\left[v_C(t_2^-) - V_a + R_a I_a^{(rest)}\right]e^{-(t-t_2)/\tau_1} + V_a - R_a I_a^{(rest)}$

Where:

$V_{crit} = (V_a - V_v)\frac{R_v}{R_a + R_v}$

$I_a^{(occl)} = I_a^{(rest)} - \frac{V_a - V_v}{R_a + R_v}$

$I_v^{(occl)} = I_v^{(rest)} + \frac{V_a - V_v - V_{ext}}{R_a + R_v}$

Table 2: *Analytical expressions for the circuit model for "large" rectangular V_{ext} ($V_{crit} \le V_{ext} < V_a - V_v$)*

	$t<t_1$	$t_1 \le t < t^*$	$t^* \le t < t_2$	$t \ge t_2$
$i_a(t)$	$I_a^{(rest)}$	$I_a^{(rest)}e^{-(t-t_1)/\tau_2}$	$\left[i_a(t^{*-}) - I_a^{(occl)}\right]e^{-(t-t^*)/\tau_1} + I_a^{(occl)}$	$\left[i_a(t_2^-) - I_a^{(rest)}\right]e^{-(t-t_2)/\tau_1} + I_a^{(rest)}$
$i_v(t)$	$I_v^{(rest)}$	0	$-I_v^{(occl)}e^{-(t-t^*)/\tau_1} + I_v^{(occl)}$	$\left[i_v(t_2^-) - I_v^{(rest)}\right]e^{-(t-t_2)/\tau_1} + I_v^{(rest)}$
$v_C(t)$	$V_a - R_a I_a^{(rest)}$	$-R_a I_a^{(rest)}e^{-(t-t_1)/\tau_2} + V_a$	$\left[v_C(t^{*-}) - V_a + R_a I_a^{(occl)}\right]e^{-(t-t^*)/\tau_1} + V_a - R_a I_a^{(occl)}$	$\left[v_C(t_2^-) - V_a + R_a I_a^{(rest)}\right]e^{-(t-t_2)/\tau_1} + V_a - R_a I_a^{(rest)}$

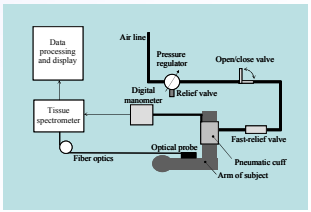

Fig. 2: Experimental Setup
The NIRS optical measurements were performed with a multi-channel frequency-domain tissue Spectrometer (OxiplexTS, ISS, Inc., Champaign, IL). The optical probe was secured on the subject's forearm. A pressure cuff was placed around the subject's upper arm. The cuff pressure was accurately controlled by a system of valves and manometers. A pressure monitor (PM015D, World Precision Instruments, Inc., Sarasota FL) permitted a digital read-out and generated an analog output which was used to synchronize the pressure readings with the NIRS data collection.

Measurement protocols

Six healthy human subjects participated in the experiments, three males and three females, 35 years of average age (range: 26-52 years; standard deviation: 9.3 years). All six subjects performed both protocols described below. The first protocol, aimed at studying the temporal features of the hemodynamic changes in the forearm in response to a 60 mmHg cuff pressure to the upper arm, was performed to validate the model predictions for the time dependence of blood volume. The second protocol, involving the application of increasing cuff pressure values, was performed to validate the model predictions for the dependence on the cuff pressure of (1) the asymptotic changes in THC and StO_2, and (2) the initial rate of increase of THC.

Results

Protocol 1: Hemodynamic response to venous occlusion
The first protocol consisted of an initial baseline acquisition (about two minutes) and the repetition for five times of the following set of procedures: (1) fast cuff inflation to 60 mmHg (inflation rate: ~20 mmHg/s), (2) maintaining the cuff pressure at 60 mmHg for 40 s, (3) fast deflation of the cuff (deflation rate: ~30 mmHg/s), and (4) maintaining the cuff deflated for 30 s. A cuff pressure value of 60 mmHg achieves venous occlusion in the upper arm.

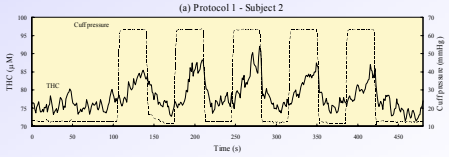

Fig. 3: *Hemodynamic response to venous occlusion The dashed lines represent the cuff pressure applied to the subject's upper arm. The continuous lines are the THC measured on the subject's forearm (brachioradial muscle).*

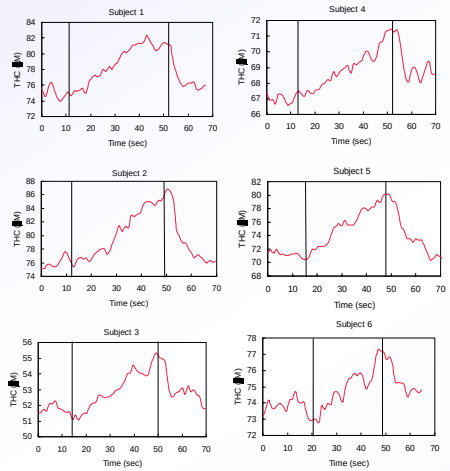

Fig. 4: *Total hemoglobin concentration (THC) measured in the forearm (brachioradialis muscle) of each of the six subjects examined during protocol 1. The vertical lines indicate the start and the end of the venous occlusion by applying a cuff pressure of 60 mmHg around the upper arm.*

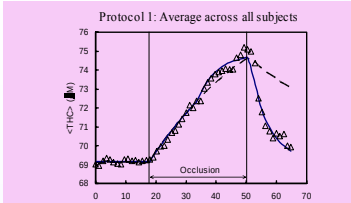

Fig. 5 *Average across all six subjects of the temporal response of total hemoglobin concentration (THC) to venous occlusion. The symbols represent the experimental data, the dashed line represents the one-time-constant model ("small" V_{ext}, where diode D is always conducting), and the solid line represents the two-time-constant model ("large" V_{ext}, where diode D is non-conducting during the initial period of occlusion).*

Protocol 2: Effect of cuff pressure
The second protocol consisted of a few minutes of baseline acquisition and the repetition of the following four steps for 11 different values of cuff pressure: (1) fast cuff inflation (~20 mmHg/s) to a given pressure value, (2) maintaining the cuff pressure for 3-5 min until the THC reached steady state (which typically occurred after ~2-3 min), and (3) quickly deflate the cuff (typically over 1-2 s). The cuff was inflated to a different value for each of the 11 repetitions of the above steps, with a range of values of 5-60 mmHg.

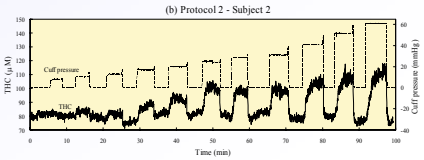

Fig. 6: *Effect of cuff pressure on the same subject as above. The dashed lines represent the cuff pressure applied to the subject's upper arm. The continuous lines are the time traces of the THC measured on the subject's forearm (brachioradial muscle).*

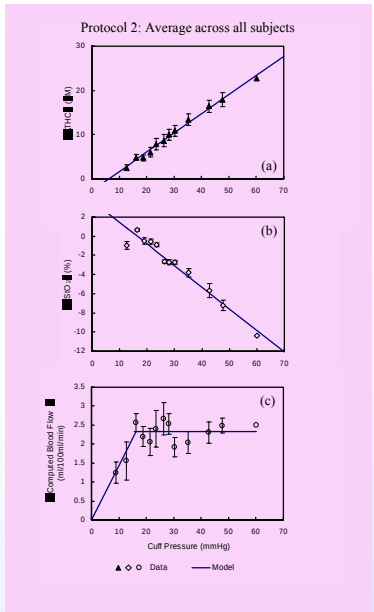

Fig. 7: *Average across all six subjects of the cuff pressure dependence for the changes induced by occlusion in: (a) total hemoglobin concentration (ΔTHC), (b) tissue saturation (ΔStO_2), and (c) blood flow computed by the initial rate of increase of THC. The symbols represent the experimental data, whereas the lines represent the qualitative model predictions, namely a linear increase in ΔTHC (panel (a)), a linear decrease in ΔStO_2 (panel (b)), and a biphasic behavior of the early slope of THC that linearly increases at low pressures while it becomes a constant at higher pressures (panel (c)).*

Discussion

Protocol 1: Hemodynamic response to venous occlusion
The experimental data of <THC> is compared with the predictions of the model for the cases of "small" V_{ext} (i.e. $V_{ext} < V_{crit}$) and "large" V_{ext} (i.e. $V_{crit} \le V_{ext} < V_a - V_v$). For this comparison, we have used the expressions for $v_C(t)$ that are reported in Tables 1 and 2. The capacitor voltage v_C is proportional to the capacitor charge, which describes the blood volume in this model. While both cases are able to describe the increase in blood volume during the time when the cuff is inflated, the fast decay toward baseline of <THC> after the cuff deflation (relative to the slower pressure-induced increase in <THC>) is only described by the case of "large" V_{ext}. This result indicates that the value of $V_{ext} = 60$ mmHg is greater than V_{crit}. The theoretical lines in Fig. 5 have been obtained by adjusting the model parameters to obtain a good agreement between the experimental data and the model. In particular, we have found that the time constant for pressure-induced increase in <THC> ($\tau_2 \sim 40$ s) is significantly greater than the recovery time constant ($\tau_1 \sim 6$ s).

Protocol 2: Effect of cuff pressure
The pressure of cuff inflation was varied for each repetition and kept for a sufficiently long time to allow the THC to reach steady state. The steady state values of ΔTHC and ΔStO_2 are predicted by the model to be linearly dependent on the cuff pressure. In fact, after defining $A = \frac{V_a - V_v}{R_a + R_v}$ and $B = \frac{1}{R_a + R_v}$, the limiting expressions for steady state (ss) v_C (which models THC) and i_v (which models StO_2) during occlusion are given by $v_C^{(ss)} = V_a - AR_a + BR_aV_{ext}$, and $i_v^{(ss)} = A - BV_{ext}$, respectively. Fig. 7(a) and 7(b) report the experimental results for the dependencies of <ΔTHC> and <ΔStO_2> (averaged across all subjects). The linear dependence of the limiting values of v_C and i_v as a function of external voltage, as well as the fact that the slope of v_C is positive and the slope of i_v is negative, are consistent with the experimental dependencies of <ΔTHC> and <ΔStO_2> on the cuff pressure.

The initial rate of increase of THC during venous occlusion (dTHC/dt at $t = t_1^+$ in our model) has been used to measure the blood flow in skeletal muscle using NIRS. For blood flow measurements, the time derivative of THC is divided by the hemoglobin concentration in blood. Our model predicts that such initial rate of increase of THC is linear with cuff pressure for the case $V_{ext} < V_{crit}$ but is independent of cuff pressure for the case $V_{crit} \le V_{ext} < V_a - V_v$. In fact, for $V_{ext} < V_{crit}$, $d\text{THC}/dt(t_1^+) = V_{ext}/(R_vC)$ whereas for $V_{crit} \le V_{ext} < V_a - V_v$, $d\text{THC}/dt(t_1^+) = (V_a - V_v)/[(R_a + R_v)C]$. Because of the continuity of v_C as a function of V_{ext}, when V_{ext} assumes the value of V_{crit} the expressions for $d\text{THC}/dt(t_1^+)$ in the two cases coincide. Fig. 7(c) shows the values of blood flow (BF) computed from the experimental data using the equation $\text{BF} = \frac{1}{K}\left.\frac{d\text{THC}}{dt}\right|_{max}$, where K is the concentration of hemoglobin in blood for which we have assumed a typical value of 2.3 mM, and we have used the maximum time derivative of THC during the first 10 s of occlusion. The experimental results of Fig. 7(c) are consistent with the model prediction of a linear behavior of the initial slope of THC as a function of cuff pressure (at small cuff pressures) and a constant value of the initial slope of THC for cuff pressures greater than a critical value, which for our data is ~18 mmHg.

Acknowledgments

This work was supported by the National Science Foundation, Award No. BES-0093840(CAREER). Thanks also go to Ning Liu for her precious assistance.

References:

1. **Westerhof, N., Elzinga G., and Sipkema P.**. An artificial arterial system for pumping hearts. *J. Appl. Physiol.* 31: 776-781, 1971
2. **Stergiopulos, N., Westerhof B., and Westerhof N.** Evaluation of methods for the estimation of total arterial compliance. *Am. J. Physiol. Heart Circ. Physiol*. 276 (1): H81-H88, 1999
3. **Olufsen, MS, Nadim A, and Lipsitz L.** Dynamics of cerebral blood flow regulation explained using a lumped parameter model. *Am J Physiol Regul Integr Comp Physiol* 282: R611-R622, 2002
4. **Voytik SL. Babbs CF. and Badylak SF**. Simple electrical model of the circulation to explore design parameters for a skeletal muscle ventricle. *Journal of Heart Transplantation. 9(2):160-74, 1990*
5. **Babbs CF. Weaver JC. Ralston SH. Geddes LA**. Cardiac, thoracic, and abdominal pump mechanisms in cardiopulmonary resuscitation: studies in an electrical model of the circulation. *American Journal of Emergency Medicine. 2(4):299-308, 1984*
6. **R Olmi, S Andreoli, M Bini, P Feroldi and L Spiazzi** An electrical model of biological tissues undergoing hyperaemia. *Phys. Med. Biol. 43 (1998) 3405–3418.*
7. **C. Casavola, L. A. Paunescu, S. Fantini, E. Gratton**. Blood flow and oxygen consumption with near-infrared spectroscopy and venous occlusion: spatial maps and the effect of time and pressure of inflation," *J. Biomed. Opt.* **5**(3), 269-276 (July 2000).
8. **Sainz, J. Cabau and V.C. Roberts** Deceleration vs. acceleration: a haemodynamic parameter in the assessment of vascular reactivity. A preliminary study. *Med. Eng. Phy., 1995, vol. 17, 91-95*
9. **S. Fantini, M. L. Hoimes, C. Casavola, M. A. Franceschini** Spatial Mapping Of Blood Flow and Oxygen Consumption in the Human Calf Muscle Using Near-Infrared Spectroscopy, Proc. SPIE **424**, 69-77 (2001)
10. **R. A. de Blasi, M. Ferrari, A. Natali, G. Conti, A. Mega, A. Gasparetto** Noninvasive Measurement of Forearm Blood Flow and Oxygen Consumption by Near-Infrared Spectroscopy," *J.Appl. Physiol*. **76**, 1388-1393 (1994)